GEOARCHAEOLOGICAL XRF LAB

ARCHAEOLOGICAL X-RAY FLUORESCENCE SPECTROMETRY LABORATORY
8100 WYOMING BLVD., SUITE M4-158 ALBUQUERQUE, NM 87113 USA

ENERGY-DISPERSIVE X-RAY FLUORESCENCE (XRF) ANALYSIS MAJOR OXIDE AND TRACE ELEMENT CONCENTRATIONS OF SILICIC METAVOLCANIC ROCK ARTIFACTS FROM THE JOHANNES KOLB SITE (38DA75) DARLINGTON COUNTY, SOUTH CAROLINA

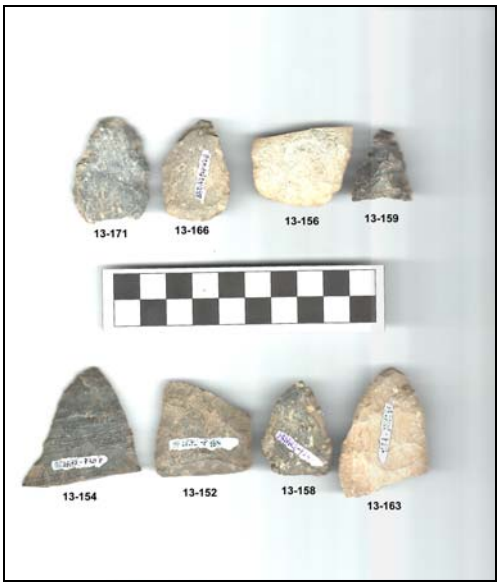

Metarhyolite biface preforms and fragments from 38DA75

by

M. Steven Shackley Ph.D., Director
Geoarchaeological XRF Laboratory
Albuquerque, New Mexico

Report Prepared for

Chris K. Young
Department of Anthropology
Eastern New Mexico University
Portales, New Mexico

3 March 2014

INTRODUCTION

The non-destructive whole rock analysis here of 105 archaeological specimens from the Johannes Kolb site in northern South Carolina indicates the procurement of stone raw materials from mainly high-silica metavolcanic rocks of Paleozoic age most likely originally from the Uwharrie Mountains of the Carolina Slate Belt to the north in North Carolina, some of which were procured from the Great Pee Dee River alluvium nearby (Horton and Zullo 1991; Rogers 2006). Compositional analysis of the tools from this site, including bifaces and fragments indicates that most of these artifacts were produced from raw materials not present in the nearby river alluvium based on the analysis of the river cobbles. Based on the compositional analysis here, the debitage, both with and without cortex appears to be a result of tool production from the local cobbles rather than the raw materials used to produce most of the finished tools at the site.

In order to aid in the determination of the source of the raw materials from which the artifacts were produced, data from the earlier analysis of metavolcanic rock from the region was included (Glascock and Speakman 2006; see also Bondar 2001). A statistical analysis of the elemental composition was used to both characterize the artifacts and cobbles from the site, and compare to the Glascock and Speakman results.

LABORATORY SAMPLING, ANALYSIS AND INSTRUMENTATION

All archaeological samples are analyzed whole. The results presented here are quantitative in that they are derived from "filtered" intensity values ratioed to the appropriate x-ray continuum regions through a least squares fitting formula rather than plotting the proportions of the net intensities in a ternary system (McCarthy and Schamber 1981; Schamber 1977). Or more essentially, these data through the analysis of international rock standards, allow for inter-instrument comparison with a predictable degree of certainty (Hampel 1984; Shackley 2011).

Trace Element Analyses

All analyses for this study were conducted on a ThermoScientific *Quant'X* EDXRF spectrometer, located in the Geoarchaeological XRF Laboratory, Albuquerque, New Mexico. It is equipped with a thermoelectrically Peltier cooled solid-state Si(Li) X-ray detector, with a 50 kV, 50 W, ultra-high-flux end window bremsstrahlung, Rh target X-ray tube and a 76 μm (3 mil) beryllium (Be) window (air cooled), that runs on a power supply operating 4-50 kV/0.02-1.0 mA at 0.02 increments. The spectrometer is equipped with a 200 l min^{-1} Edwards vacuum pump, allowing for the analysis of lower-atomic-weight elements between sodium (Na) and titanium (Ti). Data acquisition is accomplished with a pulse processor and an analogue-to-digital converter. Elemental composition is identified with digital filter background removal, least squares empirical peak deconvolution, gross peak intensities and net peak intensities above background.

The analysis for mid Zb condition elements Ti-Nb, Pb, Th, the x-ray tube is operated at 30 kV, using a 0.05 mm (medium) Pd primary beam filter in an air path at 200 seconds livetime to generate x-ray intensity Ka-line data for elements titanium (Ti), manganese (Mn), iron (as $Fe_2O_3^T$), cobalt (Co), nickel (Ni), copper, (Cu), zinc, (Zn), gallium (Ga), rubidium (Rb), strontium (Sr), yttrium (Y), zirconium (Zr), niobium (Nb), lead (Pb), and thorium (Th). Not all these elements are reported since their values in many volcanic rocks are very low. Trace element intensities were converted to concentration estimates by employing a quadratic calibration line ratioed to the Compton scatter established for each element from the analysis of international rock standards certified by the National Institute of Standards and Technology (NIST), the US. Geological Survey (USGS), Canadian Centre for Mineral and Energy Technology, and the Centre de Recherches Pétrographiques et Géochimiques in France (Govindaraju 1994). Line fitting is linear (XML) for all elements. When barium (Ba) is analyzed

in the High Zb condition, the Rh tube is operated at 50 kV and up to 1.0 mA, ratioed to the bremsstrahlung region (see Davis 2011; Shackley 2011a). Further details concerning the petrological choice of these elements in Southwest obsidians and other volcanic rocks is available in Shackley (1988, 1995, 2005; also Mahood and Stimac 1991; and Hughes and Smith 1993). Nineteen specific pressed powder standards are used for the best fit regression calibration for elements Ti-Nb, Pb, Th, and Ba, include G-2 (basalt), AGV-2 (andesite), GSP-2 (granodiorite), SY-2 (syenite), BHVO-2 (hawaiite), STM-1 (syenite), QLO-1 (quartz latite), RGM-1 (obsidian), W-2 (diabase), BIR-1 (basalt), SDC-1 (mica schist), TLM-1 (tonalite), SCO-1 (shale), NOD-A-1 and NOD-P-1 (manganese) all US Geological Survey standards, NIST-278 (obsidian), U.S. National Institute of Standards and Technology, BE-N (basalt) from the Centre de Recherches Pétrographiques et Géochimiques in France, and JR-1 and JR-2 (obsidian) from the Geological Survey of Japan (Govindaraju 1994).

Major and Minor Oxide Analysis

Analysis of the major oxides of Na, Mg, Al, Si, K, Ca, Ti, Mn, and Fe is performed under the multiple conditions elucidated below. This fundamental parameter analysis (theoretical with standards), while not as accurate as destructive analyses (pressed powder and fusion disks) is usually within a few percent of actual, based on the analysis of USGS RGM-1 obsidian standard (see also Shackley 2011a). The fundamental parameters (theoretical) method is run under conditions commensurate with the elements of interest and calibrated with four USGS standards (RGM-1, rhyolite; AGV-2, andesite; BHVO-1, hawaiite; BIR-1, basalt), and one Japanese Geological Survey rhyolite standard (JR-1). The oxides are normalized to the RGM-1 USGS recommended versus measured values.

Conditions of Fundamental Parameter Analysis[1]

Low Za (Na, Mg, Al, Si, P)

Voltage	6 kV	Current	Auto[2]
Livetime	100 seconds	Counts Limit	0
Filter	No Filter	Atmosphere	Vacuum
Maximum Energy	10 keV	Count Rate	Low

Mid Zb (K, Ca, Ti, V, Cr, Mn, Fe)

Voltage	32 kV	Current	Auto
Livetime	100 seconds	Counts Limit	0
Filter	Pd (0.06 mm)	Atmosphere	Vacuum
Maximum Energy	40 keV	Count Rate	Medium

High Zb (Sn, Sb, Ba, Ag, Cd)

Voltage	50 kV	Current	Auto
Livetime	100 seconds	Counts Limit	0
Filter	Cu (0.559 mm)	Atmosphere	Vacuum
Maximum Energy	40 keV	Count Rate	High

Low Zb (S, Cl, K, Ca)

Voltage	8 kV	Current	Auto
Livetime	100 seconds	Counts Limit	0
Filter	Cellulose (0.06 mm)	Atmosphere	Vacuum
Maximum Energy	10 keV	Count Rate	Low

[1] Multiple conditions designed to ameliorate peak overlap identified with digital filter background removal, least squares empirical peak deconvolution, gross peak intensities and net peak intensities above background.

[2] Current is set automatically based on the mass absorption coefficient.

The data from the WinTrace software were translated directly into Excel for Windows software for manipulation and on into SPSS for Windows for statistical analyses. In order to

evaluate these quantitative determinations, machine data were compared to measurements of known standards during each run. RGM-1 a USGS obsidian standard is analyzed during each sample run for obsidian artifacts to check machine calibration (Table 1).

DISCUSSION

In many ways the analysis of these artifacts with respect to assignment to source is a partial blind test. While no actual primary source rocks were available, beyond the secondarily deposited cobbles included here, it was possible to compare these data to that derived from some of the 80 regional source rocks reported by Glascock and Speakman from NAA and XRF analyses at the Missouri University Research Reactor Center (MURR; Glascock and Speakman 2006). Twenty years of comparison between laboratories, however, has indicated good agreement on trace elements, in part because both laboratories calibrate using international standards, and in this case, RGM-1, the USGS rhyolite standard. Neutron activation analysis (NAA) measures Sr, Y, Zr, Nb, and Ba poorly which are well measured incompatible elements in volcanic rocks with XRF (see Shackley 2005, 2011a). Therefore, only the XRF results from the *Stone Quarries and Sourcing in the Carolina Slate Belt* were used for comparison (Steponaitis et al. 2006; Glascock and Speakman 2006).

Research Trajectory

Given the relatively large sample, a multivariate statistical versus three-dimensional and bivariate plotting program was initiated. This has proven effective especially when the source is, in part, unknown (Glascock et al. 1998; Shackley 1998, 2007).

While all samples were analyzed for trace elements (Ti-Nb, Ba, Pb, Th), a sample of the cobbles was analyzed for oxides and plotted on a TAS diagram to determine rock type (Tables 2 and 3, Figure 1). Immediately apparent was that these rocks are likely highly metamorphosed

rhyolites (metarhyolites) where some of the alkal-feldspars have changed to quartz during metamorphosis through what is often called greenschist facies metamorphism, but can occur through hydrothermal alteration during emplacement (Ehlers and Blatt 1982; Hatch et al. 1972). This process does not take much time geologically. In southern California and northern Baja California, the Santiago Peak Metavolcanic Province exhibits similar rocks metamorphosed in similar manner, but are Jurassic in age (Balch et al. 1984; Jones and Miller 1982). Hydrothermally altered rhyolites are favored raw materials during the Clovis period in New Mexico from the quarries near Socorro and have a very similar character to samples in this assemblage (Dello-Russo 2004), and fine-grained dacites in northern New Mexico were at times selected for point production during the Folsom period (Shackley 2011b). In all these cases, and presumably the Uwharrie rhyolites, metamorphism has produced an excellent raw material for stone tool production, but at a cost geoarchaeologically. Long-term metamorphism "scrambles" the geochemistry, and sometimes creates rather extensive elemental variability including increasing silica (SiO_2), such as the case here, and variable trace element composition from one area to another (see Bondar 2011 for a regional case).

Statistical versus Geological Interpretation

In order to tease out any variability in this large sample, a cluster to discriminant analysis was first applied using Rb, Sr, Zr, Nb, and Ba as variables which appeared to be most variable in the data and were elements well above XRF detection limits. An average linking/squared Euclidean algorithm was used on the above variables in hierarchical cluster analysis (Figure 2). Cluster analysis is favored for geochemical data since it is often not multivariate normal and cluster analysis is not subject to non-normal issues (see Baxter 1992, 1994). Viewing the cluster dendrograms, one using artifact sample numbers and Glascock and Speakmans quarry (FBL) numbers, and an identical dendrogram using tool types and quarry numbers indicates that the

vast majority of artifacts and quarry data are clustered into one major cluster (digital version of the dendrograms available for clarity). Also, the tools cluster separately from the quarry and other artifacts, a result of most exhibiting very high relative barium composition, not present in the quarry data or artifacts (see Table 2 and Figure 2).

The clusters were saved as prior probabilities for discriminant analysis, and the results were similar. By using the clusters as priors in discriminant, the multivariate normality issue is avoided, or more properly "fudged" so that issues like 3pxn rule (empty cells due to too many variables relative to cases) are avoided. Tables 4-7 display the discriminant results and statistical test of the statistic. The Box's M indicates relatively well measured data, and the classification matrix indicates highly correlated classification; 96.4% correct classification for both original and jackknifed analyses (Tables 4 and 7). The plot of the first two canonical discriminant functions graphically shows the groups as identified in the cluster analysis as expected (Figure 3). Group 1 is that large group of artifacts and quarry data as identified in the cluster analysis. Group 2 is the other smaller group that includes the MURR results from some of the Chatham, Person, and Orange Counties, but not much from that identified as Uwharries quarries (Figure 2). Again, note that most of the tools recovered from the site exhibit a different elemental composition, particularly on Ba, and one could infer from a different rock source.

The three dimensional and bivariate plots of these data indicate similar groupings and clusters as the multivariate analysis, and as usual, are generally more illuminating (Figures 4-6; see Baxter 1992). Figure 4 shows a three-dimensional plot of just the artifact composition. Note that there are essentially two groups based on Nb, Rb, and Ba; the cobbles, and flakes both with and without cortex in one group, and tools in another. Figure 5 is the same plot with the MURR source data superimposed. Note that the vast majority of artifacts, other than the tools, cluster within the Uwharries source data, and some of the other county source data. There is a group of

mainly quarry data below the artifact cluster with only one tool (13-157) and one artifact (13-138) near that cluster. Again, the tools exhibit elemental compositions different from the quarry data in the MURR study. Finally, the bivariate plot of Nb and Rb (Figure 6) further indicates the elemental difference of the tools except for the one depleted in Rb (13-157). As in Figure 5, some of the Chatham County rocks based on the MURR study are near the tools. The caveat for this is discussed immediately below.

Does the statistical analysis make sense geologically? First, without source rock analyzed with this dataset, I had to rely on the MURR results. It is apparent that the tools at the Kolb site were produced from a different source than the other artifacts produced at the site, and these tools are not likely produced from Uwharrie suite rock based on the MURR analysis. Based on the MURR data is seems that many of the rocks collected from the various counties are from the same formation as Uwharrie suite rock somewhere in the Carolina Slate Belt (Rogers 2006). However, many of those rocks are somewhat elementally different from the MURR Uwharrie composition. Again, it is impossible to determine whether this is very real differences in sources, of variability within the metavolcanics in the region. Recall that metamorphosis can modify the composition significantly within one geological formation. Parenthetically, the cobbles exhibit Na and K oxides that are typical for rhyolites and don't show the "high in sodium (Na) and low in potassium (K)" values noted for rocks in the Carolina Slate Belt by Rogers (2006:12). Some of the Uwharrie suite rock analyzed by MURR do have high Na relative to K (i.e. FBL 12, 13, 43-50), again not the case with the cobbles from the site (Glascock and Speakman 2006).

Having said all that, it does appear that: 1) the vast majority of artifacts at the site were produced from local secondary deposits likely from the Uwharrie suite rock, but the tools were produced from different source rock. It seems plausible that these Early Archaic knappers came

to the site with spent and broken tools (see cover image), and re-tooled here with the local stone. This has been seen throughout North America and easily seen with obsidian artifacts and elemental compositional analysis at sources and sites (Shackley 1989, 2005).

REFERENCES CITED

Balch, D.C., S.H. Bartling, and P.L. Abbott
1984 Volcaniclastic Strata of the Upper Jurrasic Santiago Peak Volcanics, San Diego, California. In *Tectonics and Sedimentation along the California Margin*, edited by J.K. Crouch, and S.B. Bachman, pp. 157-170. Pacific Section, Society of Economic Palaeontologists and Mineralogists 38

Baxter, M.J.
1992 Archaeological Uses of the Biplot-A Neglected Technique? In *Computer Applications and Quantitative Methods in Archaeology*, edited by G. Lock and J. Moffet, pp. 141-148. BAR International Series S577, Oxford.

1994 *Exploratory Multivariate Analysis in Archaeology*. Edinburgh University Press, Edinburgh.

Bondar, G.H.
2001 Metarhyolite Use During the Transitional Archaic in Eastern North America. Paper presented at the 66th Annual Meeting of the Society for American Archaeology, New Orleans, Louisiana.

Davis, K.D., T.L. Jackson, M.S. Shackley, T. Teague, and J.H. Hampel
2011 Factors Affecting the Energy-Dispersive X-Ray Fluorescence (EDXRF) Analysis of Archaeological Obsidian. In *X-Ray Fluorescence Spectrometry (XRF) in Geoarchaeology*, edited by M.S. Shackley, pp. 45-64. Springer, New York.

Dello-Russo, R.D
2004 Geochemical Comparisons of Silicified Rhyolite from Two Prehistoric Quarries and 11 Prehistoric Projectile Points, Socorro County, New Mexico, U.S.A. *Geoarchaeology* 19:237-264.

Ehlers, E.G., and H. Blatt
1982 *Petrology: Igneous, Sedimentary, and Metamorphic*. W.H. Freeman and Co., San Francisco.

Glascock, M.D., G.E. Braswell, and R.H. Cobean
1998 A Systematic Approach to Obsidian Source Characterization. In *Archaeological Obsidian Studies: Method and Theory*, edited by M.S. Shackley, pp. 15-66. Kluwer/Academic Press, New York and Amsterdam.

Glascock, M.D., and R.J. Speakman
2006 X-Ray Fluorescence Spectrometry Data. In *Stone Quarries and Sourcing in the Carolina Slate Belt*, edited by V.P. Steponaitis, T.E. McReynolds, J.D. Irwin, and C.R. Moore, pp.

169-174. Research Report 25, Research Laboratories of Archaeology, The University of North Carolina, Chapel Hill.

Govindaraju, K.
1994 1994 Compilation of Working Values and Sample Description for 383 Geostandards. *Geostandards Newsletter* 18 (special issue).

Hampel, Joachim H.
1984 Technical Considerations in X-ray Fluorescence Analysis of Obsidian. In *Obsidian Studies in the Great Basin*, edited by R.E. Hughes, pp. 21-25. Contributions of the University of California Archaeological Research Facility 45. Berkeley.

Hatch, F.H., A.K. Wells, and M.K. Wells
1972 *Petrology of Igneous Rocks, 13th edition*. Thomas Murby & Co., London.

Hildreth, W.
1981 Gradients in Silicic Magma Chambers: Implications for Lithospheric Magmatism. *Journal of Geophysical Research* 86:10153-10192.

Horton, J.W., Jr., and V.A. Zullo
1987 An Introduction to the Geology of the Carolinas. In *The Geology of the Carolinas: Carolina Geological Society 50th Anniversary Volume*, edited by J.W. Horton, Jr. and V.A. Zullo, pp. 1-10. University of Tennessee Press, Knoxville.

Hughes, Richard E., and Robert L. Smith
1993 Archaeology, Geology, and Geochemistry in Obsidian Provenance Studies. *In Scale on Archaeological and Geoscientific Perspectives*, edited by J.K. Stein and A.R. Linse, pp. 79-91. Geological Society of America Special Paper 283.

Jones, D.A., and R.H. Miller
1982 Jurrasic Fossils form the Santiago Peak Volcanics, San Diego County, California. In *Geologic Studies in San Diego*, edited by P.L Abbott, p. 93-103. San Diego Association of Geologists Publication.

Mahood, Gail A., and James A. Stimac
1990 Trace-Element Partitioning in Pantellerites and Trachytes. *Geochemica et Cosmochimica Acta* 54:2257- 2276.

McCarthy, J.J., and F.H. Schamber
1981 Least-Squares Fit with Digital Filter: A Status Report. In *Energy Dispersive X-ray Spectrometry*, edited by K.F.J. Heinrich, D.E. Newbury, R.L. Myklebust, and C.E. Fiori, pp. 273-296. National Bureau of Standards Special Publication 604, Washington, D.C.

Rogers, J.J. W.
2006 The Carolina Slate Belt. In *Stone Quarries and Sourcing in the Carolina Slate Belt*, edited by V.P. Steponaitis, T.E. McReynolds, J.D. Irwin, and C.R. Moore, pp. 10-15. Research Report 25, Research Laboratories of Archaeology, The University of North Carolina, Chapel Hill.

Schamber, F.H.

1977 A Modification of the Linear Least-Squares Fitting Method which Provides Continuum Suppression. In *X-ray Fluorescence Analysis of Environmental Samples*, edited by T.G. Dzubay, pp. 241-257. Ann Arbor Science Publishers.

Shackley, M. Steven

1988 Sources of Archaeological Obsidian in the Southwest: An Archaeological, Petrological, and Geochemical Study. *American Antiquity* 53(4):752-772.

1989 *Early Hunter-Gatherer Procurement Ranges in the Southwest: Evidence from Obsidian Geochemistry and Lithic Technology*. Ph.D. dissertation, Department of Anthropology, Arizona State University.

1995 Sources of Archaeological Obsidian in the Greater American Southwest: An Update and Quantitative Analysis. *American Antiquity* 60(3):531-551.

1998 Gamma Rays, X-rays, and Stone Tools: Some Current Advances in Archaeological Chemistry. *Journal of Archaeological Science* 25:259-270.

2005 *Obsidian: Geology and Archaeology in the North American Southwest*. University of Arizona Press, Tucson.

2011a An Introduction to X-Ray Fluorescence (XRF) Analysis in Archaeology. In *X-Ray Fluorescence Spectrometry (XRF) in Geoarchaeology*, edited by M.S. Shackley, pp. 7-44. Springer, New York.

2011b Sources of Archaeological Dacite in Northern New Mexico. *Journal of Archaeological Science* 38:1001-1007.

Steponaitis, V..P., T.E. McReynolds, J.D. Irwin, and C.R. Moore (eds.)

2006 *Stone Quarries and Sourcing in the Carolina Slate Belt*. Research Report 25, Research Laboratories of Archaeology, The University of North Carolina, Chapel Hill.

Table 1. Recommended values for USGS RGM-1 obsidian standard and the mean and central tendency analyses from this study. ± = 1st standard deviation.

SAMPLE	Ti	Mn	Fe	Rb	Sr	Y	Zr	Nb	Ba	Pb	Th
RGM-1 (Govindaraju 1994)	1600	279	12998	149	108	25	219	8.9	807	24	15.1
RGM-1 (USGS recommended)[1]	1619±120	279±50	13010±210	150±8	110±10	25[2]	220±20	8.9±0.6	810±46	24±3	15±1.3
RGM-1, pressed powder standard (this study, n=5)	1594±69	283±6	13157±68	149±2	104±2	25±2	222±2	9±3	751±20	25±.8	18±4

[1] Ti, Mn, Fe calculated to ppm from wt. percent from USGS data.
[2] information value

Table 2. Elemental concentrations for the rock samples.

Sample	Art. Type	Ti	Mn	Fe	Zn	Rb	Sr	Y	Zr	Nb	Ba	Pb	Th
7	cobbles	3753	1658	29631	84	149	203	33	266	15	989	20	8
10	cobbles	1241	540	12382	58	61	108	38	211	8	671	18	5
11	cobbles	991	225	9653	38	72	34	46	217	11	656	12	13
18	cobbles	1085	289	14356	47	84	68	68	225	9	788	16	9
19	cobbles	1056	518	14209	59	66	43	67	228	10	627	13	18
20	cobbles	1051	265	12302	48	90	64	101	213	8	779	19	12
21	cobbles	923	264	11103	24	63	98	65	213	10	656	37	9
25	cobbles	990	236	11798	44	65	95	67	215	10	695	35	5
10-12	cobbles	1445	479	15125	63	82	125	41	215	6	806	18	9
10-15	cobbles	1050	365	13671	256	64	39	67	246	10	696	28	10
10-16	cobbles	1157	304	11980	31	51	72	59	226	8	681	23	10
10-17	cobbles	1115	372	12526	76	59	96	58	227	5	782	22	8
13-100	w/cortex	2418	423	23126	45	59	96	89	232	10	672	27	14
13-101	w/cortex	1607	295	12893	54	84	59	45	235	9	687	14	5
13-102	w/cortex	1127	232	11077	52	92	56	41	221	9	650	14	13
13-103	w/cortex	1087	215	9643	50	80	58	44	225	10	692	13	10
13-104	w/cortex	1211	223	14335	33	89	83	52	221	11	823	18	12
13-105	w/cortex	903	165	11249	23	98	41	30	178	10	852	19	12
13-106	w/cortex	1069	352	13930	29	77	131	28	182	12	781	10	13
13-107	w/cortex	1129	198	13148	25	65	42	42	194	8	535	13	6
13-108	w/cortex	1284	383	14003	61	118	100	52	222	9	729	14	12
13-109	w/cortex	1103	239	12240	54	77	68	52	213	6	551	15	17
13-110	w/cortex	1503	465	13968	33	97	100	53	273	9	653	14	15
13-111	w/cortex	1057	219	10312	47	71	65	42	213	10	703	14	7
13-112	w/cortex	1474	542	16404	50	94	82	56	238	9	853	12	13
13-113	w/o cortex	1348	285	13860	43	59	80	54	216	11	763	13	11
13-114	w/o	149	398	1474	98	67	89	53	239	11	675	20	14

	cortex	3		6									
13-115	w/o	122	250	1360	39	98	85	45	199	8	693	14	6
	cortex	5		0									
13-116	w/o	123	449	1891	45	99	43	85	280	8	737	13	13
	cortex	2		8									
13-117	w/o	143	444	1314	27	79	51	112	236	10	564	14	18
	cortex	4		7									
13-118	w/o	122	541	1552	44	116	83	65	233	6	896	14	11
	cortex	7		2									
13-119	w/o	130	386	1594	91	145	71	44	223	10	931	18	15
	cortex	4		1									
13-120	w/o	986	371	1405	47	90	90	58	232	12	648	18	11
	cortex			6									
13-121	w/o	132	473	1358	44	110	90	59	245	10	700	15	18
	cortex	6		1									
13-122	w/o	131	365	1540	33	69	106	66	222	11	625	21	8
	cortex	6		8									
13-123	w/o	140	351	1380	55	77	79	57	224	12	632	26	12
	cortex	9		0									
13-124	w/o	138	444	1253	48	77	74	52	227	10	693	20	3
	cortex	0		4									
13-125	w/o	131	473	1567	32	81	44	54	249	10	725	12	17
	cortex	3		1									
13-126	w/o	161	365	1453	57	75	49	41	236	8	808	22	3
	cortex	6		4									
13-127	w/o	102	282	1141	29	74	41	46	212	9	613	12	8
	cortex	7		2									
13-128	w/o	131	342	1515	68	80	67	57	234	8	692	16	8
	cortex	6		9									
13-129	w/o	141	427	1265	39	100	95	39	173	6	863	12	11
	cortex	5		0									
13-130	w/o	138	304	1368	34	74	101	79	223	8	631	19	9
	cortex	1		5									
13-131	w/o	101	373	1596	33	76	67	83	224	4	628	22	5
	cortex	5		9									
13-132	w/o	121	270	1543	56	86	67	63	252	10	735	15	12
	cortex	7		2									
13-133	w/o	163	408	1770	92	105	64	59	248	6	683	15	20
	cortex	9		0									
Sample	Art. Type	Ti	Mn	Fe	Zn	Rb	Sr	Y	Zr	Nb	Ba	Pb	Th
13-134	w/o	138	358	1194	34	94	73	47	240	11	737	14	9
	cortex	7		7									
13-135	w/o	111	472	1148	32	83	51	67	238	11	857	13	8
	cortex	6		8									
13-136	w/o	142	462	1413	45	128	91	63	247	12	104	13	14
	cortex	3		5							0		
13-137	w/o	101	223	1114	42	83	59	48	228	10	681	14	7
	cortex	9		0									
13-138	w/o	123	176	4856	21	34	51	47	257	6	829	15	12
	cortex	3											
13-139	w/o	135	281	1139	40	87	57	42	217	6	649	15	8
	cortex	6		2									
13-140	w/o	122	340	1616	52	74	83	58	231	3	726	18	14
	cortex	8		3									
13-141	w/o	114	229	9643	32	77	71	35	222	9	665	18	15
	cortex	0											
13-142	w/o	128	383	1541	13	73	62	50	220	11	861	32	8

	cortex	7		7	9								
13-143	w/o cortex	1114	407	12588	43	69	50	65	234	9	852	12	8
13-144	w/o cortex	1359	374	15815	53	93	102	54	228	11	599	14	11
13-145	w/o cortex	855	272	11375	40	58	70	45	218	8	601	19	6
13-146	w/o cortex	1588	385	15690	47	91	103	55	227	9	578	18	18
13-147	w/o cortex	1477	305	13607	37	58	68	55	243	8	473	17	9
13-148	w/o cortex	1268	612	17898	55	62	141	66	240	5	650	20	13
13-149	w/o cortex	1313	409	13675	59	79	70	56	214	8	668	15	7
13-150	w/o cortex	1148	403	10055	60	68	96	32	105	9	782	15	5
13-151	Tools	1875	972	30417	230	105	124	61	165	580	7	19	7
13-152	Tools	1467	531	15351	105	71	51	58	227	678	9	14	9
13-153	Tools	1415	344	13308	61	76	62	46	219	748	10	15	9
13-154	Tools	1005	378	9771	31	50	70	55	171	397	10	13	12
13-155	Tools	1938	404	21161	100	107	67	41	217	670	7	13	10
13-156	Tools	1272	367	12623	32	51	74	31	164	373	9	12	5
13-157	Tools	2904	689	35659	56	0	276	26	134	18	9	13	12
13-158	Tools	1252	386	15937	49	100	104	69	241	878	7	21	11
13-159	Tools	1327	445	14515	53	77	83	66	232	661	8	20	10
13-160	Tools	1766	436	16296	47	89	61	46	225	699	8	13	11
13-161	Tools	1886	600	20859	54	90	72	58	249	513	10	12	8
13-162	Tools	1737	570	13080	27	65	138	36	173	6	764	18	11
13-163	Tools	1679	385	15675	41	75	91	60	241	499	8	18	15
13-164	Tools	1287	302	11055	33	141	86	51	167	2607	11	15	9
13-165	Tools	1214	319	12481	43	55	49	43	230	6	457	12	12
13-166	Tools	995	222	11584	28	56	56	53	200	612	9	18	8
13-167	Tools	1137	355	12762	146	67	70	56	232	487	10	16	12
13-168	Tools	1416	400	14606	36	68	55	78	249	881	10	14	11
13-169	Tools	1702	533	11554	53	89	106	36	221	849	7	17	12
13-170	Tools	1298	434	13604	58	130	65	48	149	956	10	18	18

13-171	Tools	860	278	13731	31	98	83	63	219	591	7	16	8
13-172	Tools	1402	358	13287	37	75	83	56	243	12	656	19	10
13-3	cobbles	791	227	11361	78	77	117	45	142	8	770	14	11
13-80	w/cortex	1028	221	11813	46	73	65	38	199	8	512	14	5
13-81	w/cortex	1132	283	13168	44	94	88	45	226	4	662	16	8
13-82	w/cortex	1308	362	15338	37	82	92	60	230	5	560	15	10
13-83	w/cortex	1352	436	14418	27	91	95	32	176	10	946	13	10
13-84	w/cortex	805	300	12087	28	73	41	38	116	6	878	13	9
13-85	w/cortex	1453	312	13132	60	63	94	47	210	10	579	13	8
13-86	w/cortex	1103	219	12544	41	73	66	46	205	6	551	13	7
13-87	w/cortex	1226	366	12696	38	54	82	49	205	10	558	22	6
13-88	w/cortex	995	196	7610	19	68	49	43	183	11	760	13	9
Sample	Art. Type	Ti	Mn	Fe	Zn	Rb	Sr	Y	Zr	Nb	Ba	Pb	Th
13-89	w/cortex	1089	231	10818	29	62	43	40	219	8	569	14	9
13-90	w/cortex	1329	587	18051	57	87	101	56	241	14	600	13	11
13-91	w/cortex	1128	241	12427	33	74	65	44	224	11	643	14	10
13-92	w/cortex	1239	330	12081	28	70	38	49	228	6	552	11	7
13-93	w/cortex	1432	269	14551	55	80	80	56	248	10	811	14	11
13-94	w/cortex	1178	231	12851	35	64	63	52	233	10	648	15	16
13-95	w/cortex	1116	404	12420	44	88	50	40	232	9	704	13	9
13-96	w/cortex	1322	346	12387	35	53	46	34	208	8	363	10	10
13-97	w/cortex	1476	412	14117	50	106	130	51	229	4	647	20	12
13-98	w/cortex	1380	491	15739	39	105	48	54	241	10	744	13	16
13-99	w/cortex	2234	687	27734	67	105	56	47	212	11	1037	16	14

Table 3. Major oxides from a sample of the cobble assemblage.

SAMPLE	Na2O %	MgO %	Al2O3 %	SiO2 %	K2O %	CaO %	TiO2 %	MnO %	Fe2O3 %	Σ[1]
20	3.559	0	8.62	79.136	3.158	0.451	0.107	0.032	1.248	96.311

21	4.537	0	8.73	79.2	2.143	0.723	0.09	0.037	1.245	96.705
10-15	5.295	0	9.55	76.852	2.671	0.298	0.198	0.051	1.755	96.67
10	4.228	0.021	9.02	78.72	2.381	0.7045	0.115	1.075	1.324	97.5885
10-12	4.135	0	9.94	76.21	2.815	1.104	0.171	0.072	1.806	96.253
RGM1-S4	3.723	0.007	12.251	74.547	5.151	1.497	0.323	0.042	2.248	99.789

[1] Totals less than 100% due to absence of some major oxides and trace elements from the calculation.

Table 4. Original and jackknifed (cross-validated) classification results for the discriminant analysis.

Classification Results[a,c]

		Average Linkage (Between Groups)	Predicted Group Membership			Total
			1	2	3	
Original	Count	1	127	0	1	128
		2	1	21	4	26
		3	0	0	13	13
	%	1	99.2	.0	.8	100.0
		2	3.8	80.8	15.4	100.0
		3	.0	.0	100.0	100.0
Cross-validated[b]	Count	1	127	0	1	128
		2	1	21	4	26
		3	0	0	13	13
	%	1	99.2	.0	.8	100.0
		2	3.8	80.8	15.4	100.0
		3	.0	.0	100.0	100.0

a. 96.4% of original grouped cases correctly classified.

b. Cross validation is done only for those cases in the analysis. In cross validation, each case is classified by the functions derived from all cases other than that case.

c. 96.4% of cross-validated grouped cases correctly classified.

Table 5. Pooled within-groups matrices for the discriminant data.

Pooled Within-Groups Matrices

		Rb	Sr	Zr	Ba	Nb
Correlation	Rb	1.000	-.147	.139	.283	.321
	Sr	-.147	1.000	-.089	-.201	.215
	Zr	.139	-.089	1.000	-.354	.097
	Ba	.283	-.201	-.354	1.000	-.090
	Nb	.321	.215	.097	-.090	1.000

Table 6. Log determinants for the discriminant data.

Log Determinants

Average Linkage (Between Groups)	Rank	Log Determinant
1	5	33.098
2	5	42.465
3	5	33.128
Pooled within-groups	5	42.354

The ranks and natural logarithms of determinants printed are those of the group covariance matrices.

Table 7. Box's M results for the discriminant analysis.

Test Results

Box's M		1283.475
F	Approx.	37.719
	df1	30
	df2	4195.305
	Sig.	.000

Tests null hypothesis of equal population covariance matrices.

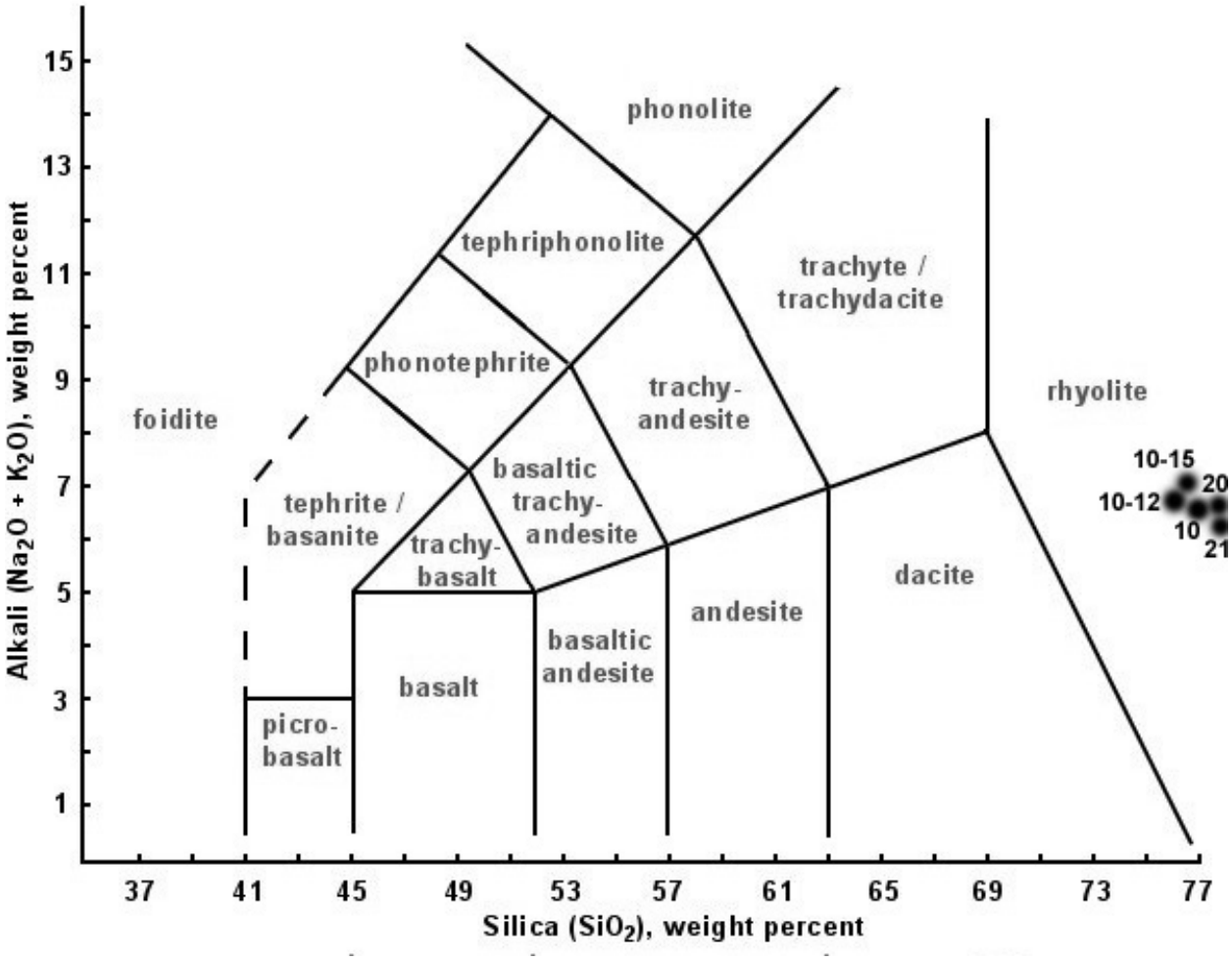

Figure 1. TAS plot of samples from the cobble assemblage.

Figure 2. Average linking, hierarchical cluster dendrograms of all data based on Rb, Sr, Zr Nb, Ba.
Left=quarry&artifact types; right=artifact numbers (13-x) and quarry designation (FBL-x) from Speakman (2006).

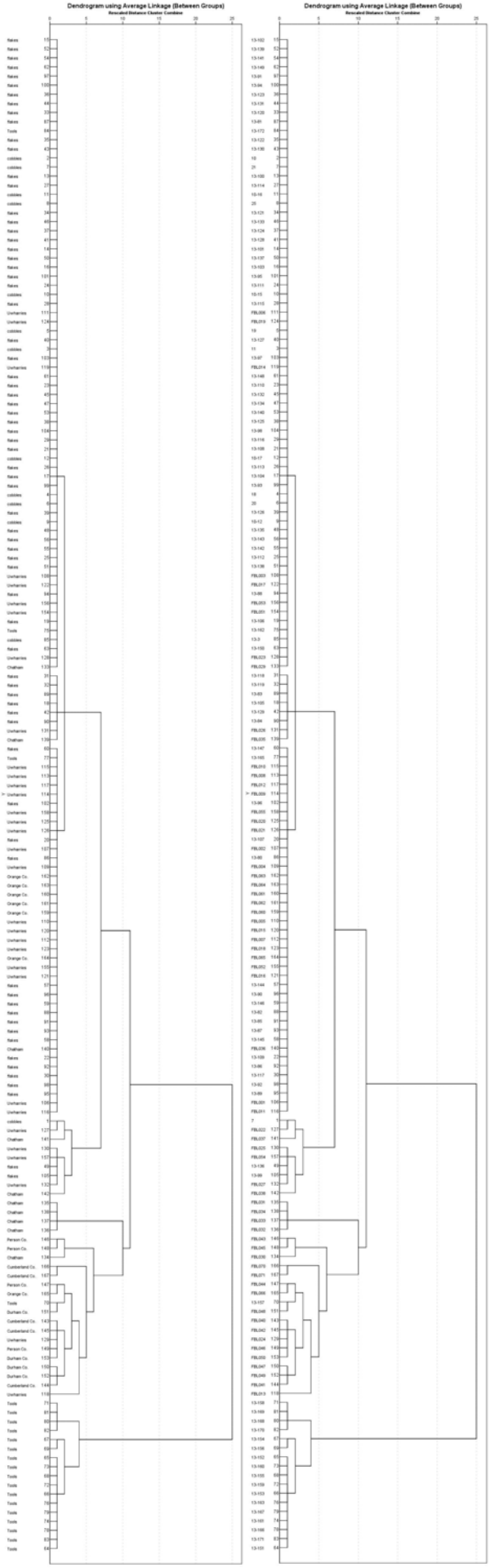

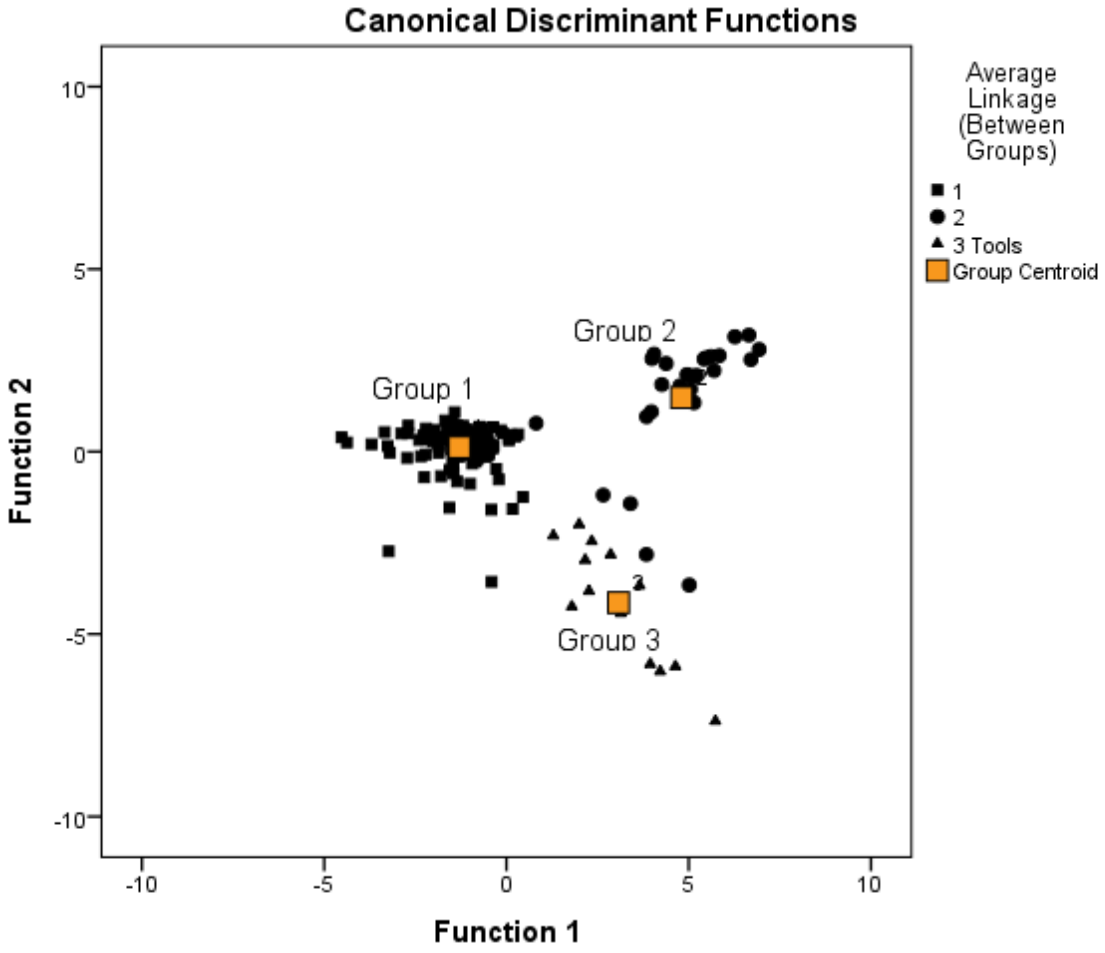

Figure 3. Plot of the first two canonical discriminant functions from the cluster groups.

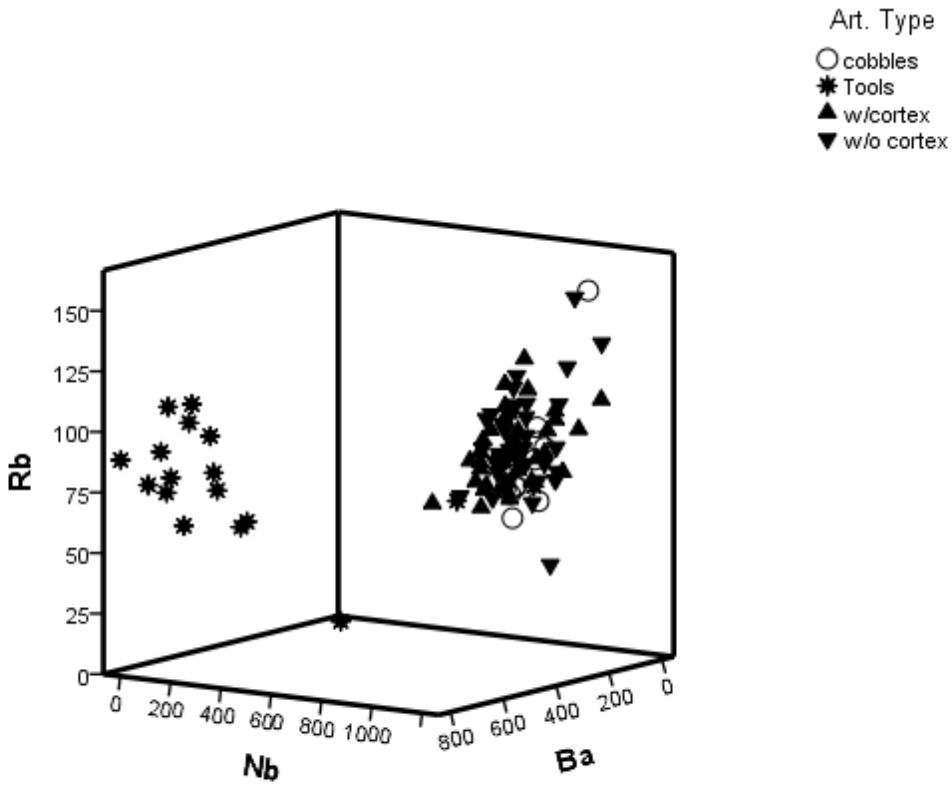

Figure 4. Nb, Rb, Ba three-dimensional plot of the artifacts only.

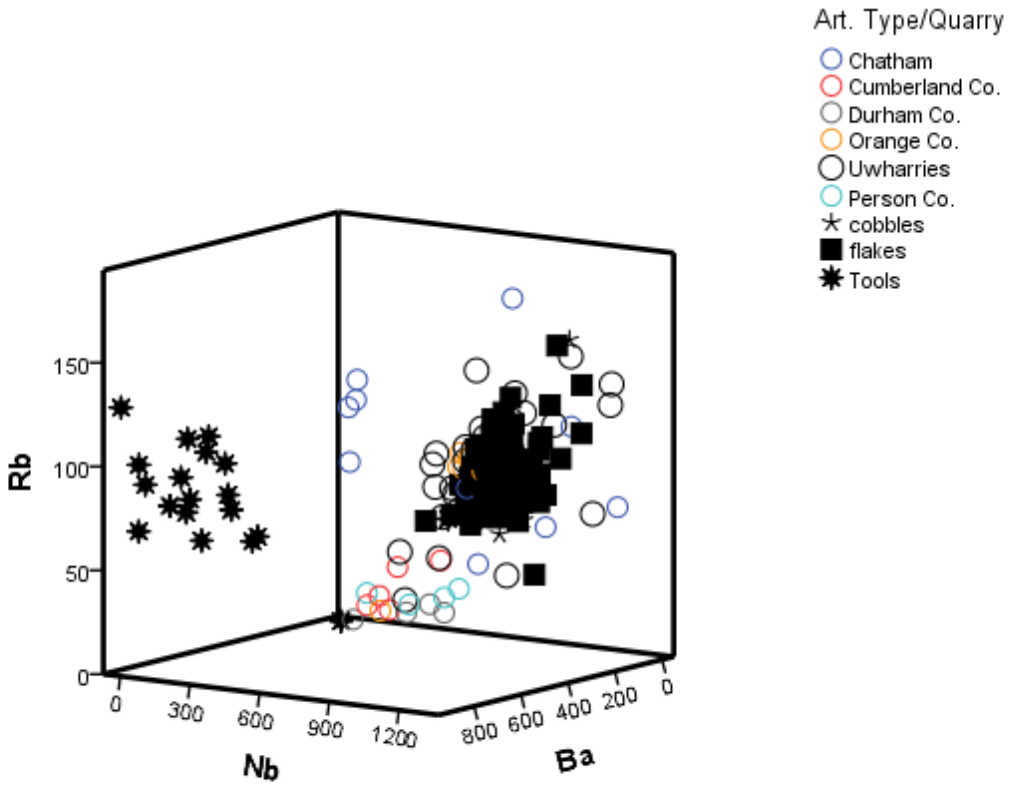

Figure 5. Nb, Rb, Ba three-dimensional plot of the artifacts and MURR source data. Compare to Figure 4.

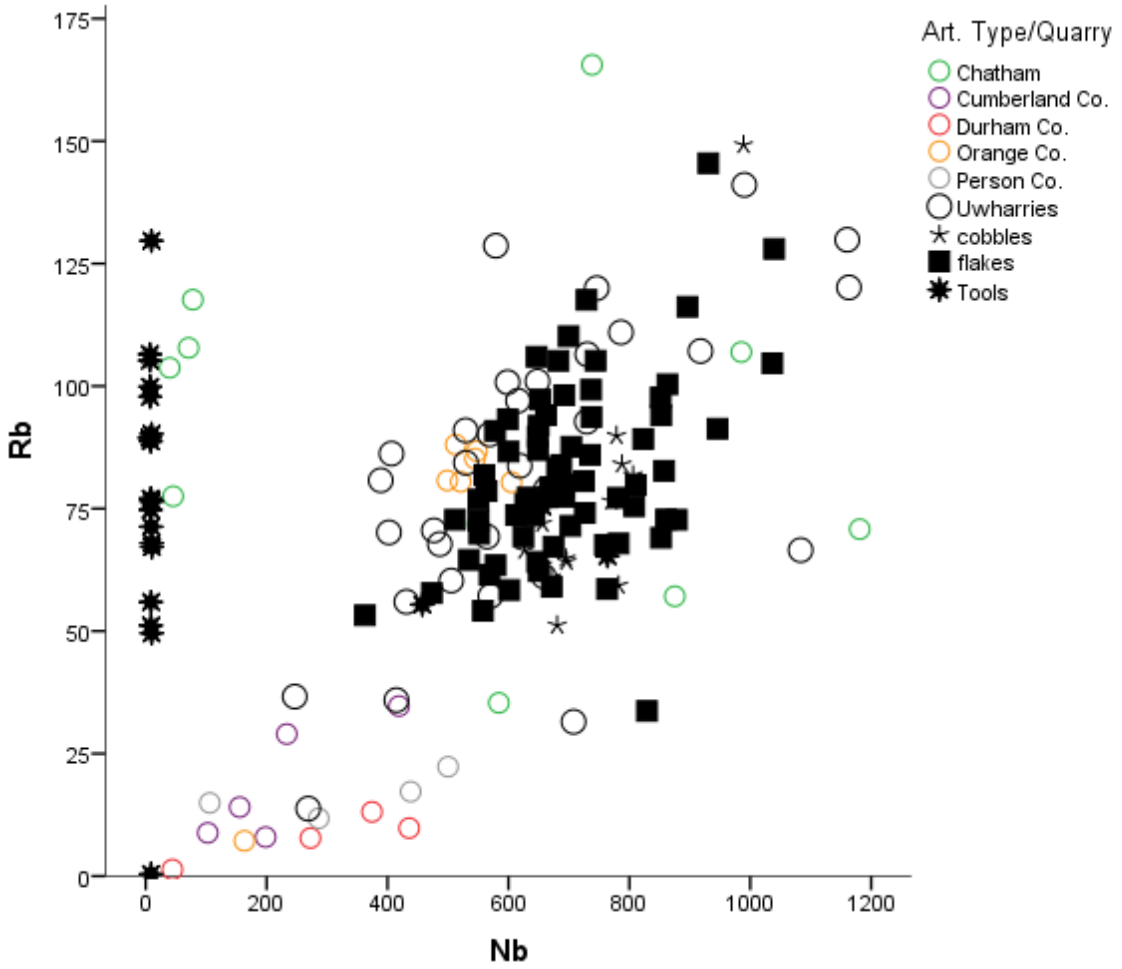

Figure 6. Nb versus Rb bivariate plot of the artifacts and MURR source data.